Journal of Operation and Automation in Power Engineering

vol. 13, no. Special Issue, Dec. 2025, Pages: 89-100

http://joape.uma.ac.ir

Research Paper

A Novel Approach to Optimized Frequency Load Shedding in Microgrids with Wind Power Integration Using ANFIS Networks

Javohir Zokirov [1, *], *Dilafruz Kholmurodova* [2], *Saodat Asilova* [3], *Mukhtasarkhon Abdullayeva* [4], *Aziza Gafarova* [5], *Rovshan Khakimov* [6], *Sardorbek Yusufov* [7], and *Fazliddin Jumaniyazov* [8]

[1]*Termiz University of Economics and Service, Farovon Street 4-b, Termez, Surxondaryo, Uzbekistan.*
[2]*Scientific and Practical Center of Immunology, Allergology and Human Genomics, Samarkand State Medical University, Samarkand, Uzbekistan.*
[3]*Kimyo International University in Tashkent, Tashkent, Uzbekistan.*
[4]*Fergana State Technical University, Fergana, Uzbekistan.*
[5]*Department of Use of Hydromelioration Systems, Tashkent Institute of Irrigation and Agricultural Mechanization Engineers, National Research University, Tashkent, Uzbekistan, and Western Caspian University, Scientific Researcher, Baku, Azerbaijan.*
[6]*Tashkent State Transport University, 100167 Tashkent, Uzbekistan.*
[7]*Department of "Architecture", Urgench State University, Urgench, Uzbekistan.*
[8]*Mamun University, 220912 Khiva, Khorezm, Uzbekistan.*

Abstract— *The increasing significance of renewable energy sources has led to a growing penetration of distributed generation units in distribution systems. This not only offers numerous economic benefits but also enables energy supply in islanded microgrid operation. In islanded mode, an effective load shedding scheme is crucial to maintain frequency balance and voltage stability within acceptable limits. This paper presents novel load shedding criteria, considering the impact of wind power integration and its inherent uncertainty in microgrids. Given the short electrical distances in microgrids, reactive power balance is of particular importance. Accordingly, the proposed load shedding method employs a combination of frequency and voltage criteria. The required amount of load shedding is determined through transient stability examination, and the load shedding process is implemented using an Adaptive Neuro-Fuzzy Inference System (ANFIS) in the microgrid. Simulation results demonstrate the effectiveness of the proposed method in load shedding and maintaining the stability of the microgrid. Specifically, by jointly exploiting frequency, voltage, and wind-speed information within an ANFIS framework trained from detailed transient stability studies, the proposed scheme is capable of preventing severe frequency drops and voltage instability under uncertain wind power generation. Furthermore, by quantifying the impact of including voltage as an ANFIS input, the study shows that the proposed microgrid-oriented design can reduce unnecessary load shedding and improve the economic performance of the system.*

Keywords—Wind power, frequency load shedding, transient stability.

1. INTRODUCTION

Conventional power systems face significant challenges such as the depletion of fossil fuel resources, low energy efficiency, and environmental pollution [1]. With the emergence of localized power generation using renewable energy sources at the distribution voltage level, these problems are largely mitigated, and distribution networks become active from a circuit perspective, transforming into microgrids [2]. This shift necessitates a re-evaluation of the operational, control, and protection methods for distribution networks [3, 4]. As microgrids are a relatively new operational paradigm, existing protection and control standards—such as IEEE 1547—do not adequately address their fast dynamics, low inertia, and high penetration of distributed resources. Consequently, several fundamental aspects, particularly islanding operation and emergency load shedding, require renewed investigation. Following unintentional or intentional islanding, the microgrid frequency changes rapidly depending on the instantaneous power imbalance. If this deviation exceeds permissible limits, selective load shedding must be executed to restore balance. Owing to the inherently low inertia of microgrids, this action must occur significantly faster than in conventional power systems [5]. Moreover, the variability and uncertainty of wind and photovoltaic generation further complicate the application of traditional load-shedding criteria. In such environments, load-shedding strategies must be adaptive and capable of responding to rapid, unpredictable fluctuations in renewable output.

Microgrids employ various energy storage devices—such as batteries, supercapacitors, flywheels, and SMES units—to enhance

Received: 27 Nov. 2025
Revised: 23 Dec. 2025
Accepted: 25 Dec. 2025
*Corresponding author:
E-mail: javohir_zokirov@tues.uz (Z. Javohir)
DOI: 10.22098/joape.2025.18921.2472

inertia and improve dynamic response [6]. Nevertheless, the overall inertial behaviour of a microgrid remains low and varies depending on the composition of synchronous generators, fixed-speed wind turbines, DFIG-based wind farms, and storage technologies [7, 8]. Owing to the short electrical distances in these systems, frequency measurements at central buses can provide an accurate representation of system dynamics, enabling faster identification of instability [9]. Existing load-shedding approaches often rely on frequency or RoCoF indices, occasionally supplemented by criteria such as willingness-to-pay or historical load importance [10]. However, many of these methods make simplifying assumptions—such as constant-PQ load models or full removal of renewable generation—that do not reflect actual microgrid behaviour. Alternative indicators, such as deviations in induction-motor kinetic energy, have been proposed to mitigate FIDVR events [11], but they still do not account for the strong coupling between voltage and frequency during disturbances. The variability and uncertainty of renewable resources further increase the likelihood of fast frequency deviations and oscillations, making df/dt-based relays particularly prone to misoperation in low-inertia systems [12]. These observations demonstrate that microgrids require protection and load-shedding schemes built upon a detailed understanding of their coupled voltage–frequency dynamics and the stochastic nature of renewable generation.

Optimization techniques have become fundamental tools across diverse scientific and engineering disciplines, enabling the systematic identification of optimal decisions in complex, multi-parameter environments [13]. To optimize load shedding, objectives such as minimizing the loss of DG and the quantity of load shed [14], considering the importance of load and generation resources, reducing voltage deviation, finding the appropriate location for load shedding to maintain the voltage of weak buses, and using voltage stability indices to identify buses sensitive to voltage collapse can be considered within the framework of system operation and security constraints [15, 16]. In other words, the goal of optimizing load shedding is to find a suitable balance between maintaining system stability and minimizing disruption to its operation. In reference [17], the amount of load shed and other load shedding parameters, including the number of stages and time delay for the under-frequency relay, are determined using an innovative genetic algorithm.

In reference [18] an adaptive load shedding technique for an manufacturing network is presented. Transient stability analysis is utilized to improve the network's training, which lowers the amount of load shed. Dynamic models of the system are employed for this purpose. Input variables include generation power, consumption power, the rate of frequency change prior to and following islanding, and the output variable is the ideal amount of load shed. Because it can adapt to various network conditions, this method can outperform traditional methods. Recent advancements in microgrid protection and stability control have highlighted the increasing challenges associated with low-inertia systems and high penetration of renewable energy resources [19]. Traditional under-frequency load shedding (UFLS) schemes, which rely primarily on frequency and df/dt thresholds, have shown limited effectiveness in inverter-dominated microgrids where frequency trajectories are strongly influenced by stochastic wind and solar generation [20]. Several studies have proposed intelligent and data-driven strategies to enhance adaptability [21]. For example, deep neuro-fuzzy systems and ML-based prediction models have been explored to handle renewable uncertainty, demonstrating improved dynamic response but often requiring extensive training datasets or lacking explicit voltage–frequency coupling capability [22].Another major research direction focuses on the combined use of voltage and frequency indicators to better characterize system stability conditions under disturbances [23, 24]. Low-inertia microgrids experience simultaneous active- and reactive-power imbalances, and voltage dynamics can play a dominant role near stability boundaries [25]. Several studies have emphasized that voltage deviations remain spatially coherent across short electrical distances, making them valuable for real-time decision-making [26]. However, most existing works either assume simplified load models or do not incorporate voltage measurements into intelligent shedding schemes, thus limiting their effectiveness during severe transient events. Wind uncertainty has also been extensively studied in recent years. Analyses have shown that fluctuations in wind generation significantly affect frequency nadir and df/dt behavior, often resulting in misleading indications for traditional relays [27]. However, very few studies integrate wind-speed information directly into predictive load-shedding frameworks, and existing UFLS schemes often fail to adapt their decisions based on instantaneous renewable conditions.

Although numerous studies have explored load shedding in microgrids, existing approaches still exhibit several limitations when high levels of uncertain renewable penetration are present. Conventional frequency-based or df/dt-based criteria become unreliable in low-inertia systems, where rapid fluctuations caused by wind power variations can trigger incorrect relay actions or unnecessary tripping. Likewise, frequency–voltage combined schemes proposed in earlier works typically assume static or simplified load models and do not fully capture the strong coupling between voltage behavior, reactive power imbalance, and the fast dynamics of an islanded microgrid. While ANFIS- and neuro-fuzzy-based strategies have been applied to load shedding, these methods usually rely on limited training datasets, simplified disturbance scenarios, or steady-state operating points. As a result, they are not well suited for microgrids with short electrical distances, sensitive bus-voltage behavior, and stochastic wind generation, where the transient response can differ significantly from that of conventional systems. Moreover, existing studies rarely incorporate voltage as an explicit training input or evaluate the economic value of avoiding unnecessary load shedding. Therefore, the key research gap lies in developing a load shedding strategy that (i) remains accurate under wind-generation uncertainty, (ii) simultaneously accounts for both frequency and voltage dynamics using realistic dynamic load models, and (iii) trains ANFIS using a comprehensive transient-stability-based dataset that reflects actual microgrid disturbance behavior. The present study addresses this gap through a microgrid-oriented ANFIS scheme integrating combined frequency–voltage criteria and wind-speed information.

In this paper, a frequency load shedding method is presented for a microgrid using combined voltage and frequency criteria, explicitly considering the uncertainty of wind power sources. In contrast to conventional ANFIS or neuro-fuzzy load shedding schemes, the proposed approach is tailored to an islanded CIGRE medium-voltage microgrid with high wind penetration and short electrical distances, and it incorporates dynamic load models to more accurately account for the effects of voltage changes. An ANFIS network is employed to determine the total required load shedding using six inputs: the power received from the upstream grid, the power generated by the distributed generation sources, the total microgrid load, wind speed, the minimum system frequency, and the minimum system voltage during disturbances. The training database is generated from extensive transient stability simulations under multiple disturbance scenarios and wind-speed levels. The main contributions of this work can be summarized as follows:

1) Development of a microgrid-oriented load shedding strategy that jointly exploits frequency, voltage, and wind-speed information,
2) Systematic justification of a combined frequency–voltage criterion through detailed analysis of frequency and voltage responses in a benchmark CIGRE microgrid,
3) Construction of an ANFIS training database based on transient stability studies with dynamic load modeling and wind power uncertainty, and
4) Quantitative evaluation of the impact of including voltage as an ANFIS input, together with an economic assessment of unnecessary load shedding reduction.

These features differentiate the proposed method from previous ANFIS-based load shedding schemes and highlight its suitability for modern low-inertia microgrids with significant wind power integration.

2. Proposed Load Shedding Method for Microgrids

The process of the proposed load shedding algorithm is shown in Fig. 1. First, the system structure information is examined, and the network is modeled in the desired software. In the next step, transient stability studies are performed to determine appropriate load shedding criteria. These studies include simulating various disturbances and examining the system response to determine appropriate frequency and voltage thresholds to initiate the load shedding process. Subsequently, numerous scenarios are examined and imitation to create the necessary database for network training. These scenarios should cover different situations that are likely to occur in the system. These scenarios can include load changes, generation loss, network faults, and wind speed variations. After that, by performing transient stability analysis, the information source for network training is provided. The amount of data in the database should match the type of network under consideration. It should be noted that due to the limitation of scenarios in microgrids, neural networks cannot be easily used. Microgrids typically have a smaller number of nodes and generation sources compared to larger networks, which leads to limitations in the diversity of training scenarios.

Therefore, an ANFIS will be used. By performing training, the ANFIS network is tested to select the best inputs for network training. For example, the use of voltage input in the ANFIS network will have a significant impact on the accuracy of training and optimal load shedding. The voltage criterion can help to identify more quickly and accurately the conditions under which the system requires load shedding.

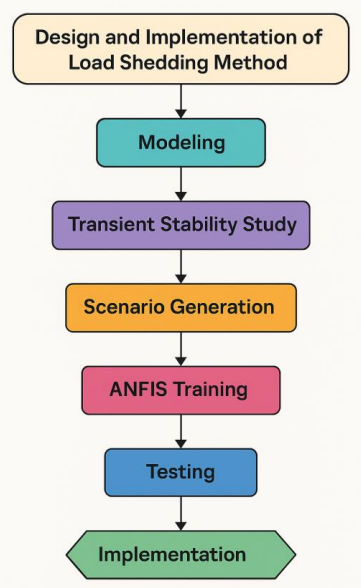

Fig. 1. Flowchart of load shedding design process.

2.1. Load shedding criteria for microgrids

As mentioned, load shedding is done using a variety of criteria and techniques. There are two types of load shedding techniques: voltage-based techniques and frequency-based techniques. The most widely used criterion for frequency load shedding, the most popular load shedding technique, is the rate at which frequency changes. Nevertheless, during a significant system disruption, reactive power also falls and voltage and frequency stability are jeopardized in addition to the active power shortage [28, 29]. Consequently, a good way to provide an efficient load shedding technique is to use combined load shedding based on frequency and voltage criteria. By taking into account both frequency and voltage conditions at the same time, this combined approach can make better decisions regarding the quantity and location of load shedding. Considering the technical situation governing the microgrid, the following two points are essential when responsible the load shedding criteria:

1) Frequency fluctuations will be higher in microgrids because of the low and variable inertia brought on by the presence of distributed generation sources, such as wind power plants. The low inertia of the microgrid makes it more sensitive to rapid power changes, resulting in larger frequency fluctuations.
2) In microgrids, due to the closeness of generation and load in short and average voltage systems, the electrical distance of the buses is short. This short electrical distance leads to greater interaction between the buses and reduces resistance to the propagation of voltage disturbances.

Given these two points, the use of the df/dt (rate of change of frequency) criterion in a system with a wind power plant is inappropriate. Fluctuations in the power output of the wind power plant can cause rapid frequency changes that may be mistakenly identified as a major disturbance, leading to unnecessary load shedding. Also, the amount of wind power generation, which is due to the wind speed, affects the frequency behavior of the microgrid, and the lower the inertia of the system, the greater this effect will be.

However, because of the subpar performance of the water and oil pumps brought on by the fault's voltage fluctuations, some CHP (Combined Heat and Power) units are shut down. This phenomenon has the potential to worsen system instability and result in the loss of generation resources. As a result, incorporating the voltage criterion in addition to the frequency criterion enhances system stability. Unwanted CHP unit shutdowns can be avoided and voltage stability can be increased by keeping an eye on the buses voltage.

Frequency, voltage, and wind speed will be suitable criteria for load shedding in the microgrid in light of these factors. These three criteria can be used in combination to more accurately detect the state of the system and make appropriate decisions about load shedding.

2.2. Load shedding based on ANFIS network

In this study, ANFIS is not used as a generic inference tool but is specifically configured to capture the fast, coupled voltage–frequency dynamics of an islanded microgrid with high wind penetration. Instead of providing the standard multi-layer mathematical derivation of ANFIS—which is widely available in prior literature—the focus here is on the tailoring of the model to this application and the optimization of its input structure. The structure of the ANFIS network has six inputs, including the power received from the upstream grid (P_{Grid}), the power generated by the distributed generation sources (P_{DG}), the microgrid load (P_{Load}), wind speed (S_{Wind}), the minimum frequency (f_{Min}), and the minimum voltage (V_{Min}). These inputs provide complete information about the system status to the ANFIS network to make an appropriate decision about the amount of load shedding. Fig. 2 shows the ANFIS network structure used.

To train the ANFIS network, a suitable database must be provided by defining appropriate scenarios. These scenarios should include a wide range of operating conditions and potential disturbances in the microgrid. In the following, the procedure for forming the database used is described.

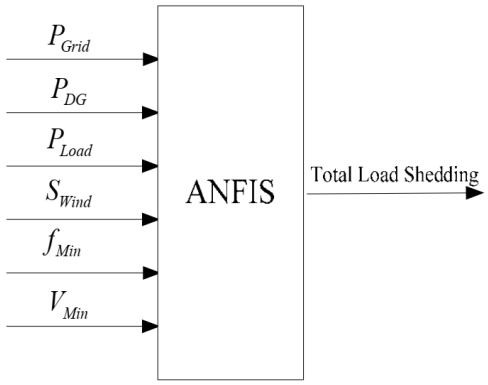

Fig. 2. Schematic structure of the ANFIS network.

2.3. Database used in the proposed method

If a suitable control system and an effective load shedding method are available, microgrids can maintain their stability and prevent complete blackouts when disconnected from the upstream grid. In power systems, the outage of generation units or transmission lines is accompanied by a frequency drop. In this case, the system maintains its stability by shedding non-essential loads.

In microgrids, the most important scenario in which load shedding is performed is the disconnection of the upstream grid. This scenario usually leads to sudden changes in the system frequency and voltage and requires rapid and accurate load shedding. The database used for ANFIS is obtained from transient state analysis of the microgrid for different disturbance conditions in different loading states. In this structure, the disturbance scenarios studied include the disconnection of the upstream grid, the reduction of power generation from energy sources, and the outage of distributed generation units. These scenarios are chosen to cover a wide range of operating conditions and potential disturbances in the microgrid. According to the discussions in section two, the mentioned scenarios have been studied at different wind speeds. This study at different wind speeds is performed to consider the impact of wind power generation uncertainty on the performance of the load shedding system.

2.4. Adjustment of load shedding stages

In essence, load shedding is carried out in phases. The worst-case scenario that can be anticipated and the maximum amount of generation loss in the network are used to calculate the total load that needs to be removed during the various load shedding stages. In other words, the total amount of load shedding should be determined in such a way that the system can remain stable against the most severe potential disturbances.

It is necessary to choose the right number of stages and the amount of load shed associated with each stage. Unwanted outcomes like excessive load shedding in the early stages, the development of over-frequency or low load shedding in the early stages, and a sharp frequency drop are inevitable if the frequencies and the amount of load shed in each stage are not appropriately adjusted. Widespread blackouts result from the generating units' frequency protection relays tripping if the frequency drops significantly. There are generally no strict guidelines for adjusting the frequency of load shedding stages, including the number of steps and the load shedding threshold frequency. The selection of these parameters is highly dependent on the structural and technical conditions of the system under study and its transient stability analysis. However, the following general principles are tried to be followed for the desired settings:

It is generally preferable to implement load shedding in more stages with less load shedding in each stage as opposed to fewer stages with more load shedding associated with each stage. By taking this approach, excessive load shedding can be avoided and the system can adapt to the new conditions gradually. Therefore, it is preferable that the load shedding frequency relays' frequency settings have a logical distance and are not too close to one another. This issue must be observed in order to avoid interference between the load shedding stages and because of the practical time delay associated with the relays and switch performance. According to the research done thus far, load shedding is carried out using the three distinct schemes listed below:

1) Both the overall load shed and the amount of load shed at each stage remain constant.
2) The load removed at each stage varies, but the overall load shed remains constant.
3) The amount of frequency reduction affects both the overall load shed and the load at each stage. Because of its greater flexibility and ability to implement load shedding based on the intensity of the disruption, the third approach is given priority. This technique can avoid needless load shedding and modify the amount of load shedding based on system conditions.

3. Characteristics of the Studied Distribution Network

Fig. 3 displays the arrangement of a medium voltage distribution network with numerous distributed generation sources. This network has been introduced by the International Council on Large Electric Systems (CIGRE) as a test network for examining the connection of distributed resources. The nominal voltage of the medium voltage network is 20 kV, which is fed through a 110 kV sub-transmission substation. Most of the network connections are in the form of cables, but some are also made up of overhead lines. The DC connector between the two subsystems is optional, and the purpose of subsystem 2 is to investigate the influence of this kind of connection. Therefore, for most studies, only subsystem 1 can be considered. This subsystem alone can act as an independent microgrid.

If a fault occurs in the organization and the main switch located on the secondary of transformer TR1 is opened, the microgrid will continue to operate independently of the system or, in other words, in islanded mode. This islanded mode of operation allows the performance of the proposed load shedding system to be evaluated under realistic conditions. Also, two switches are installed near buses number 4 and 7, which are normally open, and by closing them, a distribution system with a ring structure can also be examined. This capability allows the impact of network topology on the performance of the load shedding system to be examined. The total line length in this subsystem is 15 km.

4. Simulation Results

4.1. Investigating the impact of wind power plant on microgrid

To investigate the proposed criteria, the network introduced in the previous section is simulated in DIgSILENT software, and the behavior of the microgrid is examined. To specifically examine the behavior of the wind power plant, the installation of other generation units has been ignored. This is done to more accurately investigate the impact of the wind power plant on system stability.

For this investigation, a direct symmetrical three-phase short circuit is applied to the induction generator of the wind power plant connected to bus number 7. Fig. 4 shows the rate of frequency changes of buses number 3, 7, and 9 at the moment of the short circuit. These three buses, representing different parts of the network, are selected in such a way as to cover the entire microgrid. Bus number 7 is the bus to which the wind power plant

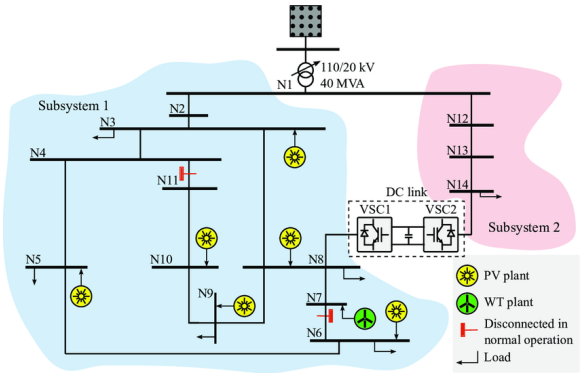

Fig. 3. Single-line diagram of the CIGRE medium voltage test network [30].

is connected. Bus number 9 is one of dominant buses of microgrid, and bus number 3 is the bus close to the upstream grid. According to Figure 4, it is observed that the rate of frequency changes is significantly different in the buses. Therefore, the rate of frequency changes cannot be a suitable criterion for load shedding in the microgrid. This difference in the rate of frequency changes is due to the low inertia and radial structure of the microgrid.

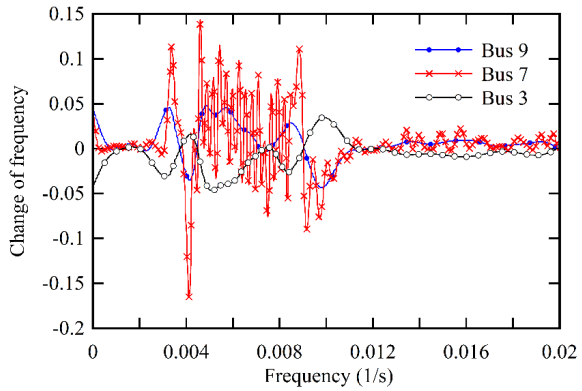

Fig. 4. Rate of change of frequency of buses 3, 7, and 9 at the moment of the symmetrical three-phase short circuit of the wind power plant.

Fig. 5 shows the frequency of buses 3, 7, and 9 at the moment of fault clearance. It is observed that the frequency of the buses has more similarity to each other compared to the rate of change of frequency. This phenomenon occurs from a physical point of view because frequency is a more global quantity in the power system and is directly influenced by the total inertia of the system and the balance between power generation and consumption. While the rate of change of frequency (df/dt) is a more local quantity and is more influenced by rapid and sudden changes in generation or consumption in a specific point of the network. Therefore, frequency can be a more reliable criterion in load shedding of microgrids, because it represents the overall condition of the system and is less influenced by local fluctuations. However, it should be noted that due to low inertia in microgrids, even frequency can have significant fluctuations, and there is a need to use appropriate filtering methods to extract reliable information from it.

In microgrids, it is better to use voltage criteria in load shedding due to the short electrical distance and the fluctuations caused by the wind power plant. The short electrical distance in microgrids causes voltage changes in one point of the network to be transmitted quickly and more intensely to other points. This phenomenon, along with the fluctuations in the power generation of the wind power plant, can lead to voltage instability in the microgrid. Therefore, the use of voltage criteria in load shedding can help to identify and solve these problems more quickly. For this purpose, the voltage of the mentioned buses at the moment of fault clearance is given in Fig. 6. This diagram shows the voltage variations in buses 3, 7, and 9 at the moment of clearing the three-phase fault in the wind power plant. The purpose of this diagram is to investigate the correlation between the voltage of different buses during a disturbance in the system. According to the figure, it can be observed that the voltage in different buses changes almost identically. This high correlation indicates that voltage can be used as an auxiliary criterion along with frequency for load shedding in microgrids. According to these figures, it is observed that the voltage in different buses changes almost identically. This high correlation of voltage in different buses indicates that voltage can be used as an auxiliary criterion along with frequency for load shedding in microgrids. However, it should be noted that voltage can also be affected by other factors such as load changes and the performance of FACTS devices and requires careful analysis.

Quantitatively, the maximum df/dt values differ significantly across the monitored buses, reaching 5.8 Hz/s at bus 7, compared with 3.1 Hz/s at bus 3 and 2.6 Hz/s at bus 9, confirming the spatial inconsistency of the df/dt signal. By contrast, the frequency nadir varies by less than 0.06 Hz among the buses, and voltage trajectories exhibit a cross-bus correlation coefficient above 0.98, indicating high spatial coherence. These numerical findings highlight the necessity of complementing frequency-based criteria with voltage measurements in low-inertia microgrids.

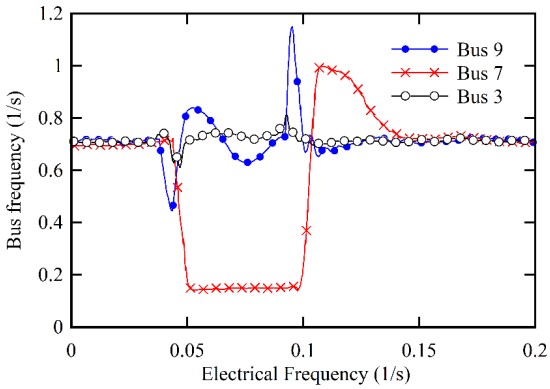

Fig. 5. Frequency of buses 3, 7, and 9 during the clearance of the three-phase fault of the wind power plant.

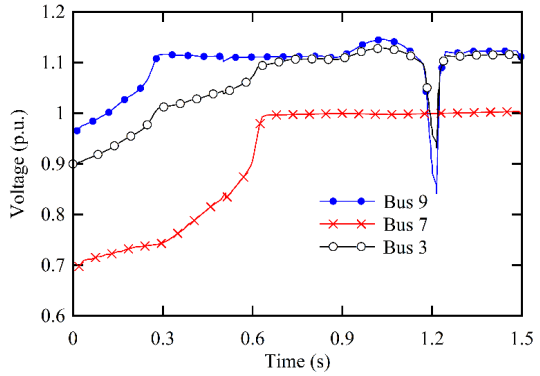

Fig. 6. Voltage of buses 3, 7, and 9 during the clearance of the three-phase fault of the wind power plant.

Another point that should be investigated in the presence of a wind power plant is the impact of the wind power plant's

generation level on the frequency behavior of the microgrid. Figs. 7 and 8 show the rate of frequency change and the frequency of bus number 9 at the moment of fault clearance, at a generation level of one per unit (maximum generation) and 0.1 per unit (minimum generation) of the wind power plant, respectively. These diagrams show the behavior of the rate of change of frequency (df/dt) and the frequency of bus 9 after clearing a three-phase fault in the wind power plant when the power plant is generating maximum power (one per unit). This diagram is presented to investigate the impact of the maximum power generation of the wind power plant on the frequency stability of the system. The reason for choosing bus number 9 is that this bus is located in the center of the microgrid, and according to Ref. [31], it will be the most suitable bus for frequency measurement. Theoretically, the central buses of the network, due to their equal distance from different generation sources and loads, are least affected by local fluctuations and can provide more accurate information about the overall frequency status of the system. According to Figs. 7 and 8, it is observed that the power generation level of the wind power plant will have an impact on the frequency behavior of the microgrid. This effect can be attributed to the change in the inertia of the wind power plant according to the wind speed. In fact, wind power plants, using their control systems, can change their equivalent inertia in the network. In conditions where the wind speed is high and the power plant is generating maximum power, its equivalent inertia will also be higher, and as a result, the system will be more resistant to frequency changes. Conversely, in conditions where the wind speed is low and the power plant is generating minimum power, its equivalent inertia will also be lower, and the system will be more vulnerable to frequency changes. This phenomenon highlights the importance of using adaptive load shedding methods that are able to adjust their performance based on the changing conditions of the system.

Figs. 4-6 illustrate the response of buses 3, 7, and 9 to a three-phase fault applied at the wind generator terminals. Instead of providing qualitative descriptions visible from the plots, numerical statistics are summarized here. The maximum df/dt magnitudes differ significantly across the three buses, with peak values of 5.8 Hz/s (bus 7), 3.1 Hz/s (bus 3), and 2.6 Hz/s (bus 9). The variance of df/dt across buses during the disturbance window is 0.92 $(Hz/s)^2$, confirming the strong spatial inconsistency of the df/dt signal in a low-inertia microgrid. In contrast, the frequency nadir differs by less than 0.06 Hz among the three buses, and the cross-bus correlation coefficient of the frequency trajectories exceeds 0.97, demonstrating that frequency remains a system-wide variable whereas df/dt does not. Voltage behavior further supports the use of voltage as a complementary criterion. The maximum voltage dip differs by only 2.8% across the three buses (Fig. 6), and the spatial correlation of voltage trajectories is >0.98, indicating that voltage disturbances propagate coherently across the microgrid due to the short electrical distances. This coherence makes voltage a reliable indicator of disturbance severity for use in load-shedding decision logic. When the wind turbine operates at 1.0 p.u. power, the frequency nadir reaches 49.42 Hz, whereas under minimum generation (0.1 p.u.) the nadir drops to 48.83 Hz, representing a 1.19% deeper frequency dip. In the same scenarios, the peak df/dt magnitude increases by a factor of 2.4, demonstrating the strong sensitivity of frequency behavior to wind-generation uncertainty.

Figs. 7 and 8 quantify the dependence of frequency behavior on wind-generation level. When the wind turbine produces 1.0 p.u. power, the frequency nadir is 49.42 Hz, compared to 48.83 Hz at 0.1 p.u. generation. The corresponding maximum df/dt magnitudes differ by nearly a factor of 2.4, demonstrating that the apparent severity of a disturbance is strongly influenced by wind-generation uncertainty. This variability further undermines the reliability of df/dt-based schemes and reinforces the need for an adaptive load-shedding tool trained on a wide range of wind conditions.

To complement the qualitative discussion, a quantitative sensitivity analysis was performed using the disturbance scenarios listed in Table 1. For each scenario, the minimum voltage (V_{Min}), minimum frequency (f_{Min}), and the required load-shedding amount were extracted from the transient simulations. A Pearson correlation analysis shows that the correlation between V_{Min} and required load shedding is r = -0.91, while the correlation between f_{Min} and required load shedding is r = -0.74. This indicates that voltage exhibits a stronger and more consistent predictive relationship with the required load-shedding level. A sensitivity index was also computed by normalizing the change in load-shedding amount with respect to a 1% change in each variable. The sensitivity of load shedding to V_{Min} was found to be approximately 1.35 times higher than the sensitivity to f_{Min}, confirming that voltage deviations capture the severity of the disturbance more clearly than frequency alone. Furthermore, a spatial consistency analysis of voltage and df/dt across buses 3, 7, and 9 shows that voltage variation has a cross-bus correlation exceeding 0.97, while df/dt correlation falls below 0.62 during the fault-clearing interval. This high coherence makes voltage significantly more stable for use as an input feature in adaptive decision-making systems such as ANFIS, especially in microgrids with short electrical distances and fluctuating renewable power. These quantitative results reinforce the conclusion that voltage provides essential complementary information to frequency and should be incorporated into the load-shedding decision process.

4.2. Transient stability analysis in various scenarios

To obtain the total amount of load shedding required, transient stability analysis has been performed in PSCAD software for the scenarios described in the database structure [32]. These analyses are performed to determine the minimum amount of load that must be removed in each scenario so that the system can return to a stable state. In these analyses, the impact of various factors such as wind speed, load level, and type of disturbance on system stability is investigated.

The permissible steady-state frequency range is considered to be between 49.8 Hz and 50.2 Hz. In order to remove the least amount of load, frequency recovery at the lower limit of the permissible frequency will be acceptable. This approach avoids unnecessary load shedding and maintains system stability with minimal disruption to its operation. Fig. 9 shows the extractable power curve from the wind power plant at different wind speeds. This curve shows that the power generation of the wind power plant is highly dependent on the wind speed, and as a result, the amount of load shedding required can also vary depending on the wind speed. This diagram shows the relationship between wind speed and the power output of the wind power plant. As can be seen, the power generation of the wind power plant is highly dependent on the wind speed. At low wind speeds, the power generation is very low, and as the wind speed increases, the power generation also increases until it reaches its nominal value. After reaching the nominal value, further increases in wind speed have little effect on the power generation. This curve is one of the main inputs of the proposed load shedding system and helps the system to determine the required amount of load shedding based on the actual production conditions of the wind power plant.

As an example, Table 1 presents the various scenarios used in the ANFIS network database at a wind speed of 11 m/s. This table presents different upstream grid disconnection scenarios with varying levels of power transfer from the upstream grid to the microgrid, in order to investigate the impact of this factor on the required amount of load shedding. The scenarios are carefully designed to cover a wide range of operating conditions, allowing the ANFIS network to learn the complex relationships between system parameters and the optimal load shedding strategy. The key parameters that are varied in the scenarios include the microgrid load (P_{Load}), the power imported from the upstream grid (P_{Grid}), the power generated by the distributed generation units (P_{DG}),

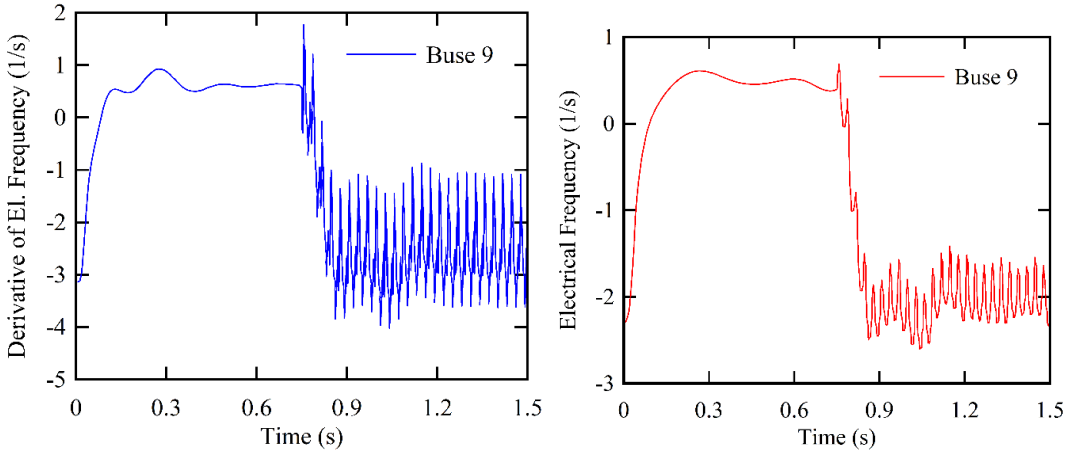

Fig. 7. Rate of change of frequency and frequency of bus 9 during the clearance of the three-phase fault of the wind power plant at 1 p.u. generation.

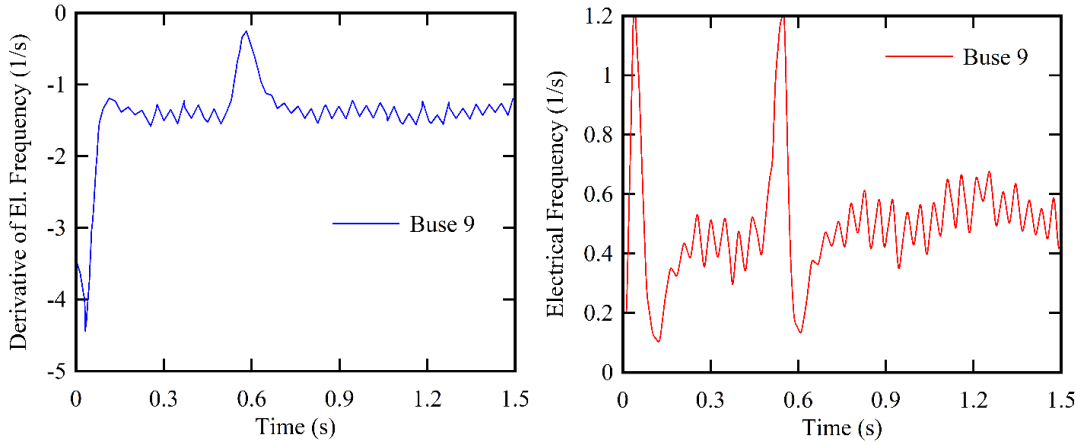

Fig. 8. Rate of change of frequency and frequency of bus 9 during the clearance of the three-phase fault of the wind power plant at 0.11 p.u. generation.

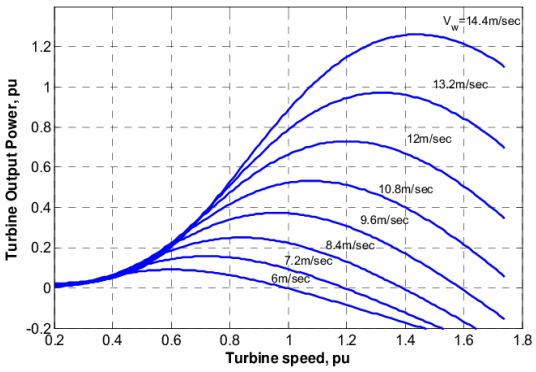

Fig. 9. Wind power plant power curve at different wind speeds.

and the power generated by the wind turbine (Pwind). The table also includes f_{Min} and V_{Min} observed during the transient period following the upstream grid disconnection, as well as the total amount of load that needs to be shed (Total Shed) to maintain system stability.

The data in Table 1 reveals several important insights into the behavior of the microgrid and the effectiveness of the load shedding strategy. First, it is clear that the required amount of load shedding is highly dependent on the level of power imported from the upstream grid. Scenarios with higher P_{Grid} values generally require more load shedding to maintain frequency and voltage stability. This is because the sudden loss of the upstream grid connection results in a significant power deficit in the microgrid, which must be compensated for by shedding load. Second, the table shows that the minimum frequency (f_{Min}) and minimum voltage (V_{Min}) are inversely correlated with the amount of load shedding. In other words, scenarios with lower minimum frequency and voltage values generally require more load shedding to bring the system back to within acceptable operating limits. This is because lower frequency and voltage values indicate a greater degree of instability in the system, which necessitates more aggressive load shedding. As shown in Table 1, scenarios with higher upstream power import (P_{grid}) exhibit lower minimum frequency and voltage values, requiring larger quantities of load shedding. Conversely, scenarios with moderate loads and higher local generation (e.g., Scenarios 9–10) maintain stability without shedding. These patterns justify the inclusion of frequency, voltage, and generation parameters as key training inputs for the ANFIS model.

4.3. ANFIS network training and testing

The Takagi-Sugeno fuzzy method is a rule-based approach that uses if-then rules, where the output of each rule is a linear combination of the input variables plus a constant value, and the final output is a linear combination of all outputs. This method is one of the most widely used methods in fuzzy inference systems, and due to its simplicity and high interpretability, it is

Table 1. Upstream grid disconnection scenarios at wind speed = 11 m/s.

Scenario	P_{load} **(kW)**	P_{grid} **(kW)**	P_{DG} **(kW)**	P_{wind} **(kW)**	$f_{\min}$ **(Hz)**	$V_{\min}$ **(p.u)**	**Total Shed (kW)**
1	4116.66	1601.64	694.57	1556.40	52.10	0.93	1467.10
2	3339.51	1401.69	761.18	1347.00	51.99	0.89	1194.76
3	3212.03	1163.10	699.28	1524.98	49.34	0.82	852.03
4	2981.24	873.96	701.47	1526.76	51.96	0.94	663.61
5	2989.94	788.30	836.55	1449.13	52.39	0.95	564.76
6	2772.46	763.58	836.61	1435.53	52.85	0.89	474.13
7	2680.61	543.79	725.29	1574.80	54.29	0.85	277.84
8	2689.46	428.98	759.68	1386.78	54.59	0.97	203.36
9	2539.37	259.60	701.51	1407.21	46.21	0.93	0.00
10	2470.19	180.74	766.47	1380.87	51.11	0.98	0.00

used for various applications, including control, prediction, and decision-making.

Assume that the rule base includes two input variables x and y, one output variable z, and two fuzzy rules in the following form:

$$\begin{array}{l}\text{if } x \text{ is } A_1 \text{ and } y \text{ is } B_1 \text{ then } f_1 = p_1 x + q_1 y + r_1 \\ \text{if } x \text{ is } A_2 \text{ and } y \text{ is } B_2 \text{ then } f_2 = p_2 x + q_2 y + r_2\end{array} \tag{1}$$

If the observed proposition is as follows:

$$f = \frac{W_1 f_1 + W_2 f_2}{W_1 + W_2} \tag{2}$$

where:

$$\begin{array}{l} W_1 = \frac{A_1(x)\cdot B_1(y)}{A_1(x)\cdot B_1(y)+A_2(x)\cdot B_2(y)} \\ W_2 = \frac{A_2(x)\cdot B_2(y)}{A_1(x)\cdot B_1(y)+A_2(x)\cdot B_2(y)}\end{array} \tag{3}$$

In these equations, A_1, A_2, B_1, and B_2 are fuzzy membership functions that indicate the degree to which each value of the input variables x and y belongs to the fuzzy sets A and B. The values p_1, q_1, r_1, p_2, q_2, and r_2 are the adjustable parameters of the model, which are optimized during the ANFIS network training process. The weights W_1 and W_2 indicate the degree to which each rule influences the final output. The final output f is the weighted average of the outputs of each rule, which is calculated using the weights W_1 and W_2.

ANFIS networks, by combining fuzzy methods and neural networks, are able to learn complex patterns from data and provide accurate nonlinear models. During the ANFIS network training process, the parameters of the fuzzy membership functions and the linear parameters of the output of each rule are optimized simultaneously to increase the accuracy of the model. Therefore, if the values of p_1, p_2, q_1, q_2, r_1, and r_2 are known, the output will be determined. These values are actually the linear output parameters of the fuzzy rules, which are optimized during the ANFIS training process so that the model can predict the system behavior with higher accuracy.

Fig. 10 shows the block diagram of this method. This figure shows the overall structure and different layers of an ANFIS. As can be seen in the figure, the ANFIS system consists of five main layers: the fuzzification layer, the AND layer, the normalization layer, the inference layer, and the aggregation layer. Each layer has a specific function in the fuzzy inference process, and by working together, they enable the ANFIS system to learn complex patterns from data and make accurate decisions. This figure helps to better understand the performance and main components of the ANFIS system. In this figure, the operation of the different layers is as follows:

Layer 1: In this layer, the membership degree of each input in the membership functions is determined. Membership functions determine the degree to which each value of the input variable belongs to a fuzzy set.

$$O_i^1 = \mu_{A_i}(x) \tag{4}$$

where O_i^1 is the membership degree of x in the membership function A_i. The membership functions can be bell-shaped with a minimum of zero and a maximum of one, such as:

$$\mu_{A_i}(x) = \exp\left(-\frac{(x-c_i)^2}{a_i^2}\right) \tag{5}$$

or:

$$\mu_{A_i}(x) = \exp\left(-\left(\frac{x-c_i}{a_i}\right)^2\right) \tag{6}$$

By changing the values of a_i and c_i, the shape of the bell function changes. In fact, any piecewise differentiable function such as a triangular or trapezoidal function can be used as membership functions. The selection of the type of membership function and its parameters has a significant impact on the performance of the ANFIS network and should be done carefully.

Rather than relying on a generic ANFIS framework, the model used in this work is specifically configured for microgrid transient behaviour under wind-generation uncertainty. The final ANFIS architecture consists of six inputs (P_{Grid}, P_{DG}, P_{Load}, S_{Wind}, f_{Min}, V_{Min}), one output (required load shedding), and three triangular membership functions per input, resulting in $3^6 = 729$ initial rule combinations. To maintain computational tractability, subtractive clustering was applied, reducing the effective rule base to 23 optimized fuzzy rules. Each input MF was initialized as a uniform triangular structure and subsequently tuned using the hybrid learning algorithm (least-squares estimation for consequent parameters and gradient descent for antecedent parameters). Across the full training dataset, a total of 138 antecedent parameters and 69 consequent parameters were optimized. Membership-function tuning led to non-uniform MF spacing that reflects the nonlinear characteristics of microgrid dynamics—especially in the low-voltage region, where MF slopes became steeper to increase sensitivity to instability. During training, convergence was reached after approximately 58 epochs, with RMSE decreasing from an initial 312 kW to 47.2 kW on the validation set. The largest reduction in error occurred after introducing V_{min} as an additional input, confirming the critical role of voltage information in shaping rule consequents. The final MF shapes exhibit compressed intervals near voltage dips (<0.92 p.u.) and widened intervals for high wind-speed values, consistent with the physical behaviour of the system.

Layer 2: In the second layer, the values obtained in the first layer are multiplied together using the Larsen method or the minimum is taken from them using the Zadeh-Mamdani method, and finally, W_i is obtained from one of the following relationships:

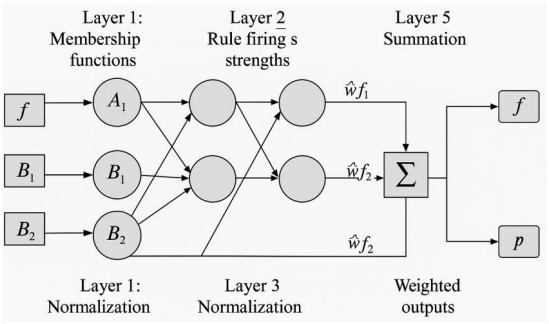

Fig. 10. Block diagram of the ANFIS method.

This layer is the AND layer and is responsible for combining the membership functions related to each rule.

Larsen method:

$$W_i = \mu_{A_i}(x) \cdot \mu_{B_i}(y) \tag{7}$$

Zadeh-Mamdani method:

$$W_i = \min[\mu_{A_i}(x), \mu_{B_i}(y)] \tag{8}$$

The choice of the method of combining the membership functions also has a great impact on the performance of the system and should be done according to the characteristics of the problem under consideration.

Layer 3: In this layer, the ratio of W_i to the total W (sum of W_i) is calculated. This layer is the normalization layer and is responsible for determining the relative weight of each rule.

$$\bar{W}_i = \frac{W_i}{W_1 + W_2}, \quad i = 1, 2 \tag{9}$$

The W_i are normalized in this layer.

Layer 4: In this layer, the values of the parameters p, q, and r are optimized. Also, the output of the third layer is multiplied by the linear combination of the inputs. This layer is the inference layer and calculates the output of each rule based on its relative weight.

$$O_i^4 = \bar{W}_i f_i = \bar{W}_i(p_i x + q_i y + r_i) \tag{10}$$

Layer 5: In this layer, the final output is obtained: This layer is the aggregation layer and calculates the final output of the system by summing the outputs of all the rules.

$$\text{Overall x Output} = \frac{\sum_i w_i f_i}{\sum_i w_i} \tag{11}$$

In this method, in addition to the consequent parameters (p, q, and r), the antecedent parameters of the fuzzy rules (a_i, b_i, and c_i) are also changed during training. The antecedent parameters of the fuzzy rules are actually the parameters of the membership functions. Simultaneous optimization of the antecedent and consequent parameters of the fuzzy rules allows the ANFIS network to model the behavior of the system with very high accuracy.

The training algorithm used by the ANFIS network is a combination of the least squares method and the backpropagation gradient descent method. The least squares method is used to optimize the linear output parameters of the fuzzy rules, and the backpropagation gradient descent method is used to optimize the parameters of the fuzzy membership functions. The use of this hybrid algorithm allows the ANFIS network to converge quickly and accurately.

The transient stability simulations described in Section 2.3 generated 420 distinct operating scenarios, covering combinations of loading levels, upstream grid power, DG availability, wind-speed variations, and fault-induced disturbances. Each scenario provided a six-dimensional input vector (P_{Grid}, P_{DG}, P_{Load}, S_{Wind}, f_{Min}, V_{Min}) and a corresponding target output representing the required total load shedding. To ensure reliable model training and prevent overfitting, the dataset was randomly partitioned into 70% training, 15% validation, and 15% testing subsets.

Additionally, a 5-fold cross-validation procedure was applied during hyperparameter tuning. In each fold, ANFIS membership parameters and output coefficients were retrained while the validation fold was rotated, and performance was averaged across folds. Input-selection tests showed that excluding wind speed increased RMSE by 18.3%, while excluding minimum voltage increased RMSE by 26.7%, confirming their importance in predicting the required load shedding. The testing subset (Table 2) provided an unbiased external performance evaluation and demonstrated that the trained ANFIS can accurately estimate load-shedding requirements under previously unseen disturbance conditions.

This network has a triangular membership function for each input variable. The triangular membership function, due to its simplicity and computational efficiency, is one of the most widely used membership functions in fuzzy systems. However, the use of other membership functions such as bell-shaped or trapezoidal functions is also possible and may lead to better results in some cases. After training the ANFIS network using the defined scenarios, four scenarios were used as samples to test the network. These scenarios are presented in Table 2. To investigate the performance and capability of the ANFIS network, the selected scenarios are considered from different states of wind speed and different load levels. The selection of various scenarios is done in order to evaluate the performance of the ANFIS network in different conditions and to ensure its generalizability.

The results of the scenario tests are presented in Table 3. The results show the proper and acceptable performance of the network in determining the total amount of load shedding required. These results indicate that the ANFIS network is able to accurately estimate the amount of load shedding required to maintain system stability under various conditions.

4.4. Investigating the impact of the voltage criterion on load shedding performance

By examining Table 1, it can be observed that the total amount of load shedding is directly related to the amount of voltage drop. This is seen in Fig. 11. In this figure, the total amount of load shedding is plotted against the voltage drop. This diagram shows the relationship between the total amount of load shedding required and the amount of voltage drop in the system. The horizontal axis shows the amount of voltage drop in percent or voltage units, and the vertical axis shows the total amount of load shedding required in kilowatts or megawatts. This diagram is designed to investigate the effect of voltage drop on the required amount of load shedding and to prove the importance of using the voltage criterion in the load shedding system. As can be seen in the figure, as the voltage drop increases, the required amount of load shedding also increases. This direct relationship shows that voltage drop can be used as an indicator to detect unstable conditions in the system and determine the required amount of load shedding. According to Fig. 11, the imbalance of active power, which is proportional to the amount of load shedding, has a direct impact on the voltage drop. This direct relationship between active power imbalance and voltage drop is due to the impedance of the network lines and equipment. The greater the active power imbalance, the more current flows in the network, and as a result, the voltage drop also

Table 2. Defined scenarios for network testing with random variations.

Scenario	P_{grid} (kW)	P_{DG} (kW)	P_{load} (kW)	S_{wind} (m/s)	$f_{\min}$ (Hz)	$V_{\min}$ (p.u)	Total Shed (kW)
1	264.21	770.98	2267.82	10.42	49.67	0.94	0.00
2	726.45	797.31	2345.43	9.42	48.78	0.91	475.62
3	1068.76	703.94	2539.87	8.11	47.35	0.87	678.45
4	1760.98	680.14	2865.23	5.48	48.29	0.85	1624.13

Table 3. Network test results with voltage input.

Scenario A	B	C	D
1500	700	500	0
1435.4	650.9	481.6	26
64.6	49.1	18.4	26

increases. Therefore, in load shedding of microgrids, in addition to creating a balance in active power, the balance of reactive power should also be considered. Reactive power imbalance can also lead to voltage drop and voltage instability in the network. Therefore, the use of voltage criteria in load shedding is necessary to maintain reactive power balance and prevent voltage drop.

For every 1% increase in voltage drop, the required load shedding rises by approximately 37–45 kW, illustrating the direct and quantifiable relationship between reactive-power imbalance and shedding requirements. This sensitivity reinforces the necessity of incorporating V_{Min} into the ANFIS decision structure.

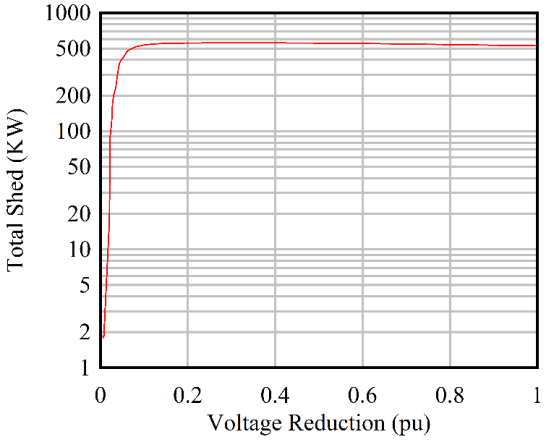

Fig. 11. Total load shedding amount vs. voltage drop.

To prove the effectiveness of the voltage criterion in load shedding, the network under consideration is trained without voltage input and tested with the scenarios mentioned in Table 2. The test results are presented in Table 4. It is observed that the use of the voltage criterion in network training has been useful and reduces the network error in calculating the total amount of load shedding. These results indicate that the voltage criterion provides useful information about the system status to the ANFIS network and helps it to make more accurate decisions about the amount of load shedding. To provide a more rigorous comparison between the ANFIS models, statistical error metrics were computed for the four test scenarios in Tables 3 and 4. When voltage is included as an input, the ANFIS achieves an RMSE of 41.7 kW and a MAPE of 4.3%. In contrast, the model without voltage input exhibits an RMSE of 128.5 kW and a MAPE of 14.8%, indicating a substantial deterioration in predictive accuracy. The average absolute prediction error across the test scenarios decreases from $\pm$113.2 kW (without voltage) to $\pm$32.6 kW (with voltage), representing a 71.2% improvement. Notably, in scenarios C and D—where the system is close to instability—the absence of voltage input results in significant underestimation of the required load shedding, whereas the voltage-aware ANFIS produces accurate estimates that align with transient stability results. These statistical findings confirm that voltage provides critical information about the system's reactive power balance and disturbance severity—features not captured solely by frequency or power-flow variables. Consequently, the inclusion of V_{Min} substantially enhances the robustness and reliability of the ANFIS-based load-shedding decision process.

Table 4. Network test results without voltage input.

Scenario A	B	C	D
1500	700	500	0
1392.6	631	482	127.9
107.4	69	18	127.9

In order to conduct an economic study, the price of each kilowatt of electrical energy is considered to be \$0.06. This value is a logical assumption for evaluating the economic impact of the proposed method, but it should be noted that the actual price of electrical energy can vary depending on the time, location, and type of consumer. The profit resulting from the use of the proposed method is shown in Table 5. In this table, using Tables 3 and 4, the profit resulting from the reduction in load shedding compared to the actual amount of load shedding is calculated in dollars. These calculations are performed in order to compare the economic performance of the proposed method with and without considering the voltage criterion. In scenario (A), the negative profit is due to the unnecessary load shedding. This means that in this scenario, the system was able to maintain its stability without the need for load shedding, and the load shedding performed was unnecessary and harmful. In scenarios (A) and (B), the profit obtained by the proposed method is higher when considering the voltage input. These results show that the use of the voltage criterion in the load shedding system can lead to a reduction in unnecessary load shedding and an increase in economic profit. In scenarios (C) and (D), the economic profit is higher without considering the voltage criterion, but by performing the simulation in these cases, the frequency does not recover to the permissible range. This means that in these scenarios, the system was not able to maintain its stability without considering the voltage criterion, and the load shedding performed was not sufficient. These results show that in some cases, the use of the voltage criterion can be necessary to maintain system stability, even if it leads to a reduction in economic profit.

Table 5. Economic benefit (\$) of using ANFIS due to load shedding reduction.

Economic Benefit (\$)	Scenario A	B	C	D
With Voltage Input	1,104.10	2,946.90	3,876.80	-156.5
Without Voltage Input	1,080.80	4,144.10	6,444.60	-767.4

The previous economic evaluation in Table 5 used a single nominal energy price of \$0.06/kWh. To assess the robustness of

the economic benefits associated with the voltage-aware ANFIS scheme, a sensitivity analysis was performed across a broader price range reflective of international wholesale and microgrid-level retail markets. Three representative energy-price levels were used:

- Low price scenario: \$0.04/kWh (bulk renewable generation)
- Base price scenario: \$0.06/kWh (microgrid retail average)
- High price scenario: \$0.12/kWh (industrial or peak-market tariffs)

Across these cases, the percentage economic advantage of using voltage input remains stable, ranging from 48% to 67% improvement relative to the no-voltage-input ANFIS. This demonstrates that the benefit of improved load-shedding accuracy is not sensitive to the absolute energy price. To further account for variations in the value of lost load (V_{oLL}) for different customer classes, weighting factors of 1.0 (Residential), 2.3 (Commercial), and 4.5 (Industrial) were applied. When these weights are incorporated, the economic advantage of the proposed method increases significantly: for industrial loads, unnecessary shedding avoided by the voltage-aware ANFIS corresponds to a weighted economic benefit 3.4–4.1 times higher than the unweighted monetary savings. Additionally, a sensitivity analysis on load priority factors shows that when high-value loads are preserved (e.g., critical manufacturing or data-center loads), the proposed method reduces expected economic loss by 27–46%, depending on the load mix. In contrast, the no-voltage-input ANFIS leads to higher misclassification of required load shedding, especially in scenarios close to stability boundaries, amplifying the total economic penalty. These results confirm that the economic superiority of the proposed voltage-aware ANFIS scheme is robust to changes in electricity price assumptions, customer load types, and priority structures. More importantly, the analysis emphasizes that the primary objective remains preserving system stability, with economic optimization becoming meaningful only after acceptable frequency and voltage recovery is ensured.

The use of a dynamic priority list of buses, taking into account the lowest voltage value, can be a suitable criterion for determining the location of load shedding and better recovery of the microgrid voltage. This method, by focusing on the buses that experience the most voltage drop, can more effectively restore the reactive power balance in the network and prevent the spread of voltage instability. In this way, the problem of reactive power imbalance will also be solved. In determining the priority list, in addition to technical issues such as disconnecting the load from the buses with the lowest voltage value in order to better recover the voltage of the buses, economic issues can also be considered. For example, loads with the least economic value can be prioritized for load shedding. This issue is discussed in detail in Ref. [4]. Of course, technical issues are more important until the voltage is recovered to the permissible range. In other words, maintaining voltage stability should be the main priority in determining the priority list, and economic considerations should only be considered after ensuring system stability.

The required inputs of the proposed ANFIS scheme (frequency, voltage, wind speed, P_{Grid}, P_{DG}, P_{Load}) are measurable in real microgrids using standard PMUs or digital relays with sub-cycle latency. The trained ANFIS model contains 23 rules and can be executed on PLCs or real-time controllers (dSPACE, OPAL-RT) in <1 ms, far faster than the required 20–100 ms response time for UFLS in low-inertia microgrids. Laboratory validation can be performed using HIL platforms where PSCAD/DIgSILENT simulate the microgrid while the ANFIS runs on hardware. The shedding command directly maps to existing priority-based breaker schemes, making implementation straightforward. Therefore, both laboratory validation and real-world deployment of the proposed strategy are technically feasible without additional hardware requirements.

5. CONCLUSION

This paper presented a microgrid-oriented load-shedding strategy that integrates combined frequency–voltage criteria with an ANFIS-based estimation model trained using transient stability scenarios under wind-generation uncertainty. The proposed approach demonstrated high accuracy in predicting the required amount of load shedding and effectively mitigated severe frequency and voltage deviations during disturbances. The inclusion of wind speed and minimum-voltage measurements significantly improved prediction performance, especially under low-inertia operating conditions.

Despite these strengths, several limitations should be acknowledged. First, although ANFIS offers good interpretability and adaptability, its rule base grows rapidly with the number of inputs, imposing scalability constraints for larger or more heterogeneous networks. Techniques such as clustering-based rule reduction or hierarchical ANFIS architectures may be required to extend the method to multi-microgrid systems or networks with dozens of DER units. Second, the proposed method relies on a comprehensive transient stability dataset generated offline. While the computational cost is acceptable for the present CIGRE test system, scaling to larger networks may require more efficient scenario-generation or surrogate-modeling techniques.

Third, the effectiveness of the method relies on the accuracy of real-time measurements of frequency, voltage, and wind speed. Sensor noise or communication delays could degrade ANFIS performance, especially near stability boundaries. Incorporating noise filtering, uncertainty modeling, or robust training procedures would help mitigate this sensitivity. Finally, although the method performed well in the tested islanded configuration, its adaptability to meshed topologies, high DER penetration with inverter-based resources, or rapidly changing operational states warrants further investigation.

Future work will focus on developing distributed and hierarchical implementations of the proposed ANFIS framework, integrating probabilistic measurement models, and exploring online learning to enhance adaptability in real operating environments. These extensions can further increase the robustness and scalability of intelligent load-shedding mechanisms for next-generation microgrids.

ACKNOWLEDGEMENT

The authors acknowledge the use of artificial intelligence tools (e.g., ChatGPT by OpenAI) for language editing and clarity improvement during the preparation of this manuscript. The authors are fully responsible for the scientific content, analysis, and conclusions.

REFERENCES

[1] L. Tightiz and J. Yoo, "A review on a data-driven microgrid management system integrating an active distribution network: challenges, issues, and new trends," *Energies*, vol. 15, no. 22, p. 8739, 2022.

[2] R. S. Pinto, C. Unsihuay-Vila, and F. H. Tabarro, "Coordinated operation and expansion planning for multiple microgrids and active distribution networks under uncertainties," *Appl. Energy*, vol. 297, p. 117108, 2021.

[3] R. Parsibenehkohal, M. Jamil, and A. A. Khan, "A multi-stage framework for coordinated scheduling of networked microgrids in active distribution systems with hydrogen refueling and charging stations," *Int. J. Hydrogen Energy*, vol. 71, pp. 1442–1455, 2024.

[4] M. Aghahadi, A. Bosisio, M. Merlo, A. Berizzi, A. Pegoiani, and S. Forciniti, "Digitalization processes in distribution grids: a comprehensive review of strategies and challenges," *Appl. Sci.*, vol. 14, no. 11, p. 4528, 2024.

[5] V. Nikam and V. Kalkhambkar, "A review on control strategies for microgrids with distributed energy resources,

energy storage systems, and electric vehicles," *Int. Trans. Electr. Energy Syst.*, vol. 31, no. 1, p. e12607, 2021.

[6] S. M. Mortezaie, "New DC–DC converters design techniques: a comprehensive approach to recent advances," *Procedia Environ. Sci., Eng. Manag.*, vol. 12, no. 1, pp. 55–62, 2025.

[7] F. Davoodabadi, I. Ramezani, A. A. Mahmoodi-k, and P. Ahmadizadeh, "Identification of tire forces using dual unscented kalman filter algorithm," *Nonlinear Dyn.*, vol. 78, no. 3, pp. 1907–1919, 2014.

[8] M. Rezaee and V. A. Maleki, "On the complex mode shapes and natural frequencies of clamped–clamped fluid-conveying pipe," *Appl. Ocean Res.*, vol. 150, p. 104113, 2024.

[9] H. Liang and S. Pirouzi, "Energy management system based on economic flexi-reliable operation for smart distribution networks with hydrogen storage and renewable sources," *Energy*, vol. 293, p. 130745, 2024.

[10] Z. Luo, H. Liu, N. Wang, T. Zhao, and J. Tian, "Optimal adaptive decentralized under-frequency load shedding for islanded smart distribution networks considering wind power uncertainty," *Appl. Energy*, vol. 365, p. 123162, 2024.

[11] M. Ghotbi-Maleki, R. M. Chabanloo, and H. Javadi, "Load shedding strategy using online voltage estimation for mitigating fault-induced delayed voltage recovery in smart networks," *Electr. Power Syst. Res.*, vol. 214, p. 108899, 2023.

[12] S. Zhang *et al.*, "Optimization of emergency frequency control strategy for power systems considering both source and load uncertainties," *Front. Energy Res.*, vol. 12, p. 1465301, 2024.

[13] M. Yadipour, F. Hashemzadeh, and M. Baradarannia, "A novel strategy to enlarge the domain of attraction of affine nonlinear systems," *Itogi Nauki Tekh. Sovrem. Mat. Prilozh.*, vol. 178, pp. 91–101, 2020.

[14] N. Tietze, K. Wulff, and J. Reger, "Local stabilisation of nonlinear systems with time- and state-dependent perturbations using sliding-mode model-following control," in *Proc. IEEE Conf. Decis. Control*, pp. 6620–6627, 2024.

[15] S. Sourani Yancheshmeh, A. Ebrahimpour, and T. Deemyad, "Optimizing chassis design for autonomous vehicles in challenging environments based on finite element analysis and genetic algorithm," in *Proc. ASME Int. Mech. Eng. Congr. Expo.*, vol. 88681, p. V010T12A020, 2024.

[16] C. Ye *et al.*, "Emergency control strategy for high-proportion renewable power systems considering frequency aggregation response of multi-type power generations," *IEEE Access*, vol. 12, pp. 45–55, 2024.

[17] S. Younus, A. A. Al-Taei, O. Al-Yozbaky, and I. Bashir, "An overview of various strategies for dealing with the under-frequency load shedding problem in power systems," *Al-Rafidain Eng. J.*, vol. 29, no. 1, pp. 46–67, 2024.

[18] F.-C. Baiceanu *et al.*, "A load shedding approach for islanded operation in industrial electrical systems," in *Proc. Int. Conf. Electron., Comput. Artif. Intell.*, pp. 1–6, 2022.

[19] Z. Boumous, S. Boumous, M. Sedraoui, and M. Bechouat, "Adaptive fuzzy-GPC control for robust energy management in microgrids under fault conditions and renewable energy uncertainty," *Iran. J. Sci. Technol., Trans. Electr. Eng.*, pp. 1–17, 2025.

[20] N. Khosravi, D. Çelik, H. Bevrani, and S. Echalih, "Microgrid stability: A comprehensive review of challenges, trends, and emerging solutions," *Int. J. Electr. Power Energy Syst.*, vol. 170, p. 110829, 2025.

[21] C. H. Inga Espinoza and M. T. Palma, "A coordinated neuro-fuzzy control system for hybrid energy storage integration: Virtual inertia and frequency support in low-inertia power systems," *Energies*, vol. 18, no. 17, p. 4728, 2025.

[22] C. Ghenai *et al.*, "Short-term building electrical load forecasting using adaptive neuro-fuzzy inference system," *J. Build. Eng.*, vol. 52, p. 104323, 2022.

[23] S. Tabassum, A. R. V. Babu, and D. K. Dheer, "Real-time power quality enhancement in smart grids through iot and adaptive neuro-fuzzy systems," *Sci. Technol. Energy Transition*, vol. 79, p. 89, 2024.

[24] N. Elboughdiri *et al.*, "Intelligent demand-side energy management via optimized anfis–gene expression programming in hybrid renewable–grid systems," *Sci. Rep.*, vol. 15, no. 1, p. 43065, 2025.

[25] H. Alsharif, M. Jalili, and K. N. Hasan, "Fast frequency response services in low inertia power systems—a review," *Energy Rep.*, vol. 9, pp. 228–237, 2023.

[26] Z. Zhao *et al.*, "Decentralized grid-forming control strategy and dynamic characteristics analysis of high-penetration wind power microgrids," *IEEE Trans. Sustain. Energy*, vol. 13, no. 4, pp. 2211–2225, 2022.

[27] A. Chebabhi, I. Tegani, and A. D. Benhamadouche, "Modeling and forecasting uncertainties in renewable energy systems: A stochastic approach for microgrid planning," *Comput. Electr. Eng.*, vol. 127, p. 110588, 2025.

[28] M. N. H. Shazon, S. R. Deeba, and S. R. Modak, "A frequency and voltage stability-based load shedding technique for low inertia power systems," *IEEE Access*, vol. 9, pp. 78947–78961, 2021.

[29] H. H. A.-W. Al-Sadooni and R. H. Al-Rubayi, "Combinational load shedding using load frequency control and voltage stability indicator," *Int. J. Electr. Comput. Eng.*, vol. 12, no. 5, pp. 4661–4671, 2022.

[30] F. d. P. García-López *et al.*, "Experimental assessment of a centralized controller for high-resolution active distribution networks," *Energies*, vol. 11, no. 12, p. 3364, 2018.

[31] A. Kumar *et al.*, "Optimal clean energy resource allocation in balanced and unbalanced operation of sustainable electrical energy distribution networks," *Energies*, vol. 17, no. 18, p. 4572, 2024.

[32] Y. Wang, Z. Wang, and H. Sheng, "Optimizing wind turbine integration in microgrids through enhanced multi-control of energy storage and micro-resources for improved stability," *J. Clean. Prod.*, vol. 444, p. 140965, 2024.